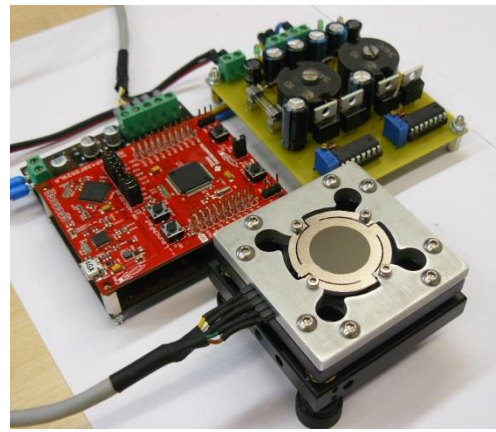


Texas Instruments Innovation Challenge: Europe Design Contest 2015 Project Report

# Piezoelectric deformable mirror

<b>Team Leader:</b>	Jaka Pribošek <a href="mailto:jaka.pribosek@fs.uni-lj.si">jaka.pribosek@fs.uni-lj.si</a>
<b>Team Members:</b>	Matija Brumat, <a href="mailto:matija.brumat@fs.uni-lj.si">matija.brumat@fs.uni-lj.si</a>
<b>Advising Professor:</b>	Prof. dr. Janez Diaci, <a href="mailto:janez.diaci@fs.uni-lj.si">janez.diaci@fs.uni-lj.si</a>
<b>University:</b>	University of Ljubljana, Slovenia
<b>Date:</b>	31.7.2015

Qty.	TI Part Number & URL	Qty.	TI Part Number & URL
1	<a href="#">MSP430F5529LP</a>	1	<a href="#">LMZ35003</a>
1	<a href="#">DAC8734</a>	1	<a href="#">LMZ34002</a>
1	<a href="#">ISO7240C</a>	2	<a href="#">TPS7A4701</a>
4	<a href="#">OPA454</a>	1	<a href="#">TPS7A3301</a>
1	<a href="#">REF02</a>	2	<a href="#">UC3525A</a>
1	<a href="#">UA78L05</a>		



**Project abstract:** The report outlines the development of low cost deformable mirror system for high precision beam steering applications. We present complete instructions how to fabricate and assemble piezoelectric deformable mirror as well as detailed description of applied analog design principles used in piezo driver and required power supply units. The driver consists of microprocessor controlling DAC whose output is amplified through HV amplifier. This way, four channel piezo mirror is powered up to 93 Vp-p at 16 bit resolution and fast 75000 points/second performance. Excellent system performance in terms of accuracy and linearity has been found. The beam steering performance was verified in a prototype optical instrument. As a result, the TI logo smaller than thickness of a human hair has been drawn with a laser.

## 1. Introduction and motivation

According to the World Health Organization, 90% of the world's visually impaired population live in countries with lower social-economic standard. Effective early diagnose of glaucoma (causing blindness), can only be achieved by an *adaptive retinal ophthalmoscope* capable of imaging through aberrant eyes. Similarly, aberrations induced by air turbulences limit the astronomers from seeing the *details in deep space*. Opposite in scale, imaging of the *smallest details at microscopic* levels has not been possible until Nipkow spinning disc microscopes appeared. Other complicated alternative beam steering concepts such as Risley prisms or Acoustooptical Deflectors are exploited to manipulate atoms using *optical tweezers*, fabricate next generation lab-on-chips using *laser lithography* or burn malignant cells using *high-end endoscopic laser scalpels* in minimal invasive surgeries. Despite the diversity of the aforementioned applications, they are all unified by the need for fast and precise light manipulation. We present a design concept that opens a flexible alternative to suit all those needs – an **ultralow cost piezoelectric deformable mirror**. Such inexpensive mirrors may open the access to high quality ophthalmoscopes for doctors in rural areas and third world countries. Further on, such mirrors can upgrade homemade telescopes of amateur astronomers to allow better observation of the planets in our universe. They can simplify and lower the cost of laser steering in the most demanding applications– they may change the design of optical tweezers and lower the complexity of laser scanning microscopes. Such mirrors open possibilities of wavefront control in laser interference lithography in order to fabricate the tinniest details at submicron levels. At fabrication costs of only few dollars, they offer an excellent disposable solution in minimal invasive laser surgery in order to avoid sterilization and thereby minimize time and costs. The beauty of it is that fabrication of both the piezoelectric deformable mirror and the mirror control electronics may be easily accomplished at home, even without access to high-tech equipment. Thanks to the integrated solutions of Texas Instruments, the big potential of deformable mirrors is now opened to many enthusiasts worldwide. ***So go, be creative and revolutionize the world!***

## 2. Theoretical background

The deformable mirror is a composite device of thin metal diaphragm, with layer of piezo ceramics on the back side and thin front-surface mirror on the front side. In such design, a diaphragm itself is common to all electrodes, what enforces the need for a single ended ground referenced excitation. Applying high positive voltage to piezo ceramics deforms the diaphragm and forms a diverging output beam (Fig.1A).

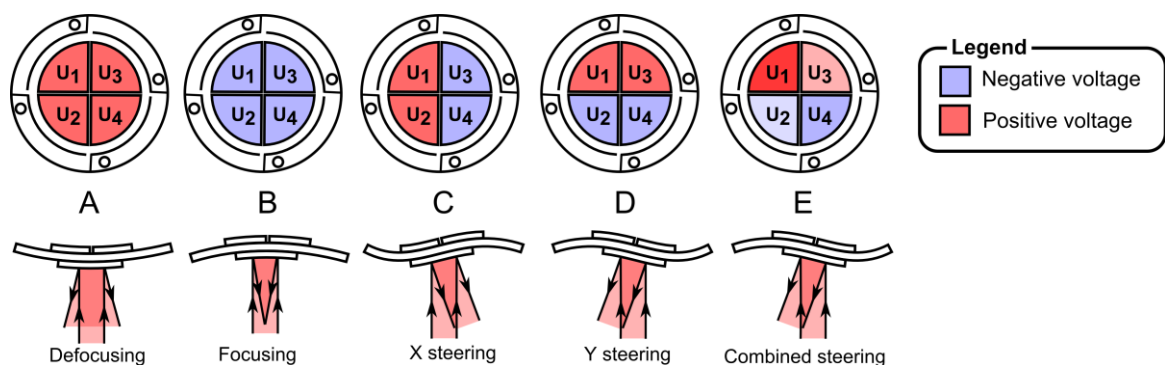


Figure 1: Concept of deformable mirror – beam focusing (A,B) and steering (C,D,E)

By reversing the voltage mirror deforms to a convex shape forming a converging output beam (Fig.1B). In case of segmented electrodes, varying voltage amplitudes between segments enforces different local curvatures of the diaphragm in a such way that two additional in-plane mirror rotations are feasible (Fig.1 C & D). Voltage differences between left and right channels result in deflection of laser beam in X direction, and differences between channels upper and lower channel deflects the laser in Y direction. This allows a combined deflection (Fig1. E) by a superposition of required electrode voltages using the following simple relationships:  $U_1 = \gamma_1(-\theta + \varphi)$ ,  $U_2 = \gamma_2(-\vartheta - \varphi)$ ,  $U_3 = \gamma_3(\vartheta + \varphi)$  and  $U_4 = \gamma_4(\vartheta - \varphi)$ , where  $\gamma_{1..4}$  are electrode sensitivity coefficients. In a typical beam steering solution, a  $1^\circ$  angular working range and frequencies up to 3 kHz are required. To allow even larger deflection angles, additional cuts in diaphragm are made to serve as flexible mounting arms, see Fig.1.

### 3. Implementation

#### 3.1 Fabrication of deformable mirror

We fabricated deformable mirrors from easily accessible low-cost piezo buzzers. The fabrication involves several consecutive steps presented in Fig.2. Buzzers are first coated with acrylic paint on both sides and patterned using 80W Nd:YAG laser. With piezo layer facing upwards, both electrodes and mounting arms were marked in one laser pass. Alternatively, a desired pattern may be scored using a carbide tip on a CNC or by hand. Next, the mounting holes and the flexible arms, integrated into diaphragm were machined using an *electrochemical machining*. Here, an anode is connected to the stainless steel diaphragm and cathode is connected to some sacrificial stainless steel plate. Then, both electrodes are dipped into salt-water solution (20 g salt in 1 L of water). By limiting the current to 0.5 A the machining through 0.15 mm stainless steel is done in cca 5 min. After machining, the paint is stripped using acetone and the wires are hand soldered to silver electrodes. A 0.12 mm thin microscopic glass slide has been grinded into a circular shape using a Dremel rotary machine with diamond wheel. Then, the glass slides were coated with chromium by an industrial grade Balzers triode sputtering system. Alternatively, for home use, chemical silvering using silver nitrate can be employed to coat the glass with thin reflective film. Once the mirror is fabricated, it is glued to the patterned piezo diaphragm with epoxy resin. Next, the mirror was mounted on a dedicated aluminium mount fabricated on a homemade CNC machine.

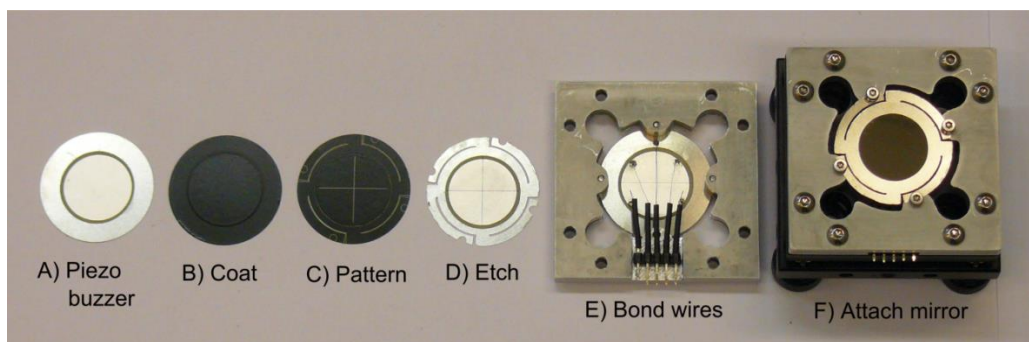


Figure 2: Consecutive steps of mirror fabrication.

### 3.2 System architecture

Generally, a curvature of a bimorph piezo actuator is proportional to amplitude of applied voltage. To achieve deflections that deform the surface of the mirror to an useful degree, several tens of volts may be necessary. Fast driving of capacitive loads is governed by equation of electrical reactance given by  $x_c = 1/(2\pi fC)$ , which for piezo buzzers used in our design (resonant frequency at  $f=3.5$  kHz and  $C=60$  nF) results in  $760 \Omega$ . Solely driving this load at 3.5 kHz and 100 Vp-p amplitudes requires a 3.3 W HV power supply, not including quiescent currents of the amplifier and supply itself. Conventional bipolar switching designs regulate only positive voltage where negative remains unregulated. Using such power supply in an asymmetrically loaded application may result in swinging output voltage at the unregulated rail which can easily damage the HV amplifier. To solve this, a regulation of both rails is required. For this purpose a custom HV split-rails switching converter is developed based on two separate **UC3525A** in a push-pull topology.

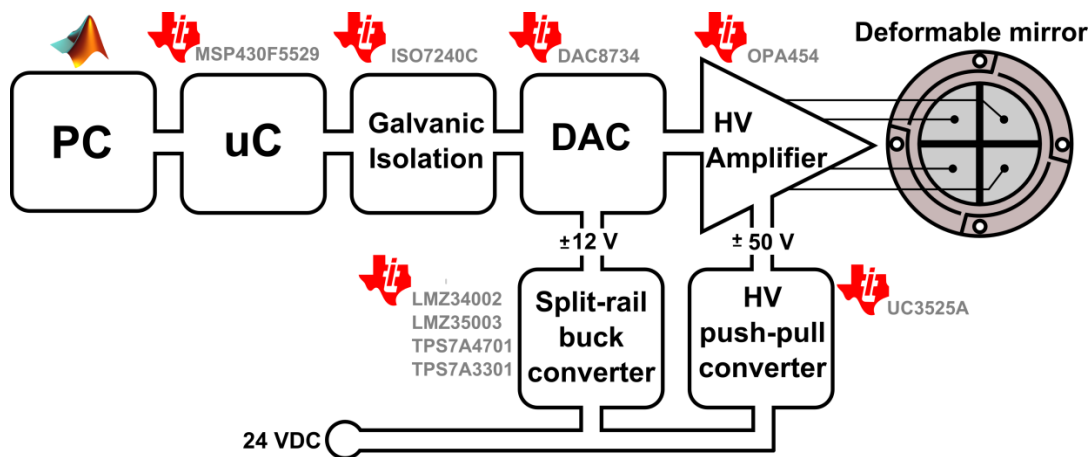


Figure 2: Complete system architecture

To drive a piezoelectric actuator, integrated haptic drivers such as DRV8662 or DRV2700 would normally be a preferred choice as they simplify the design with their integrated boost converter and easy-to-use interfaces. Unfortunately, bimorph deformable mirror enforces a single ended ground referenced architecture, which prevents the use of differential architecture as used in DRV series drivers. Instead, we used a bipolar DAC to generate required signals and amplify the signals by an additional high voltage amplifier. Optimal design solution has been found by a combination of quad channel precision **DAC8734**, offering 16 bit resolution and  $\pm 10$  V signal amplitude, fast SPI interface and synchronous channel update, with **OPA454** offering 50 mA output at widest output voltage swing in their class. This way fast, precise and stable operation is guaranteed by choosing the appropriate TI components.

To maintain a 16 bit output precision, an ultra-low noise  $\pm 12$  V power supply is required to power DAC. We used a regulated split-rail buck converter built with **LMZ35003** and **LMZ34002** power modules to lower the input voltage at  $\pm 13$  V. Each rail is then regulated by ultra-low noise LDOs (**TPS7A4701** and **TPS7A3301** for positive and negative rail respectively) in order to provide optimal voltage stability for precision DAC. Finally, to prevent any possible damage, a galvanic isolation of 4 SPI data lines is employed – due to high frequency signals (24 MHz Clock) a high speed capacitive digital isolator **ISO7240C** was used.

A chosen heart of the piezo driver is **MSP430F5529 Launchpad** due to 24 MHz

clock, high speed USB, plenty of powerful timers, DMA features, JTAG debug capabilities and most of all an extremely steep learning curve thanks to numerous examples provided by TI.

Lastly, **Mathworks Matlab** was chosen as a primary platform throughout the development stage, as it allows data acquisition, signal generation and analysis under the same roof. As such, plenty of room for further research towards numerical modelling is left opened.

### 3.2.1 High voltage push-pull converter

To avoid troubles due to asymmetric loads, as discussed in chapter 3.2, a split-rail DC-DC power supplies based on two TI **UC3525A** regulators in a push pull design topologies was built. We chose an operating frequency of a 20 kHz, for which a ferrite pot-core custom transformer with 2.08 ratio (50 V/24 V=2.08) was designed and built. Both coils are made from CuL 0.35 mm<sup>2</sup> wire to suit the general rule of a thumb 3 A/mm<sup>2</sup>. The number of primary winds is given by an equation  $N = (U_{primary} 10^4) / (K_f B_{max} f A_e)$  with  $K_f = 4$  for square wave signals,  $A_e$  for Ø26x16 pot-core is 94 mm<sup>2</sup> and  $B_{max}$  set as 0.15 T. We thus wound 11 bifilar winds on primary and 28 bifilar winds on secondary side to suit the voltage ratio and account for 20 % output voltage reserve for PWM and voltage drops. 100 V IRF540 N-channel MOSFET transistors with low  $R_{dsON} = 40\text{ m}\Omega$  are used. A 12 V Zener is used to drop  $V_C$  and keep the FET's  $V_{gs}$  voltage under 20 V. A 10 uF capacitor provides soft start in 0.5 s. Ultra-fast rectifying diodes UF4007 and low pass LC filter (L1 and C16) with a cut-off frequency at  $\frac{1}{2\pi\sqrt{LC}} = 112\text{ Hz}$  serve for smooth DC output voltage.

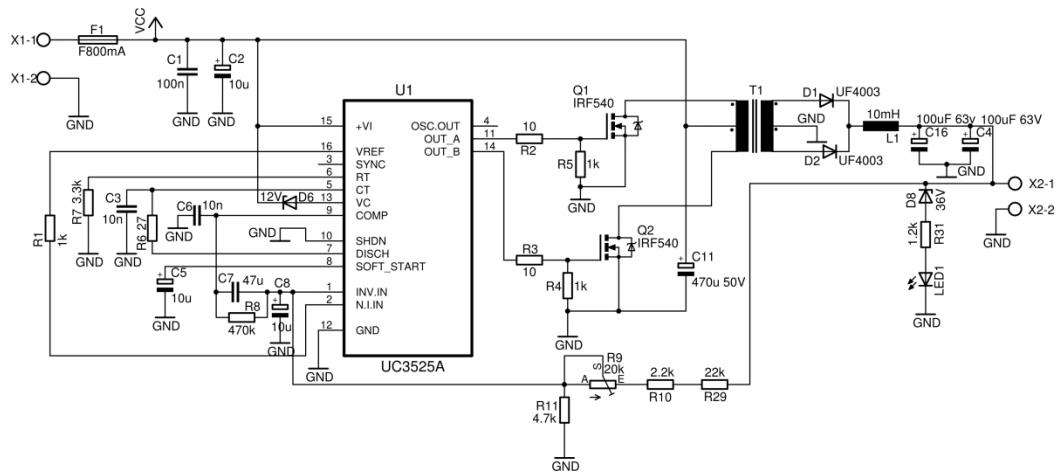


Figure 3 : Push-pull positive voltage rail

Conceptually, a negative rail is similar to the positive one presented in Fig.3. In order to trick the UC3525A to control a negative output, an unconventional solution is made at the input of the error voltage amplifier (Fig.4). A voltage divider (R12, R25, R26) is used to apply 3 V bias to the negative feedback input. Positive input is biased at 5.1 V through R24 which allows the UC3525A to start. Negative feedback, which drives inputs of error amplifier in equilibrium, is provided by R27. The PCB was organized symmetrically for both rails. Massive ground plane was created, and higher loaded traces have been kept 100 mils wide. HV push-pull power supply was



designed as a single sided PCB, so it can be easily fabricated at home. Here, a combination of 0805 SMD components and through-hole components was found to be an ideal solution for creation of small footprint PCB and lower the number of air-wires (Fig 4: right).

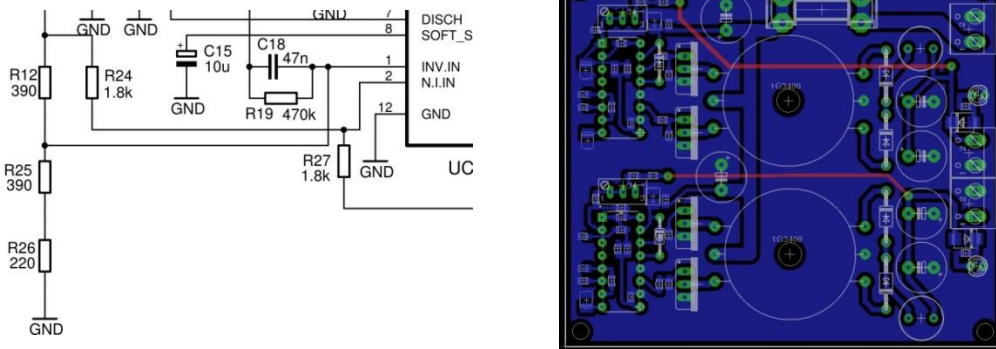


Figure 4: Negative voltage rail design variation at the input of error voltage amplifier (left), and complete PCB layout of a converter (right).

### 3.2.2 Split-rail buck converter

First, to prevent any possible damage, the design involves a simple safety circuit including input overvoltage and polarity protection. This is implemented by a P-FET followed by a 2 W 36 V Zener diode (Fig.5 A).

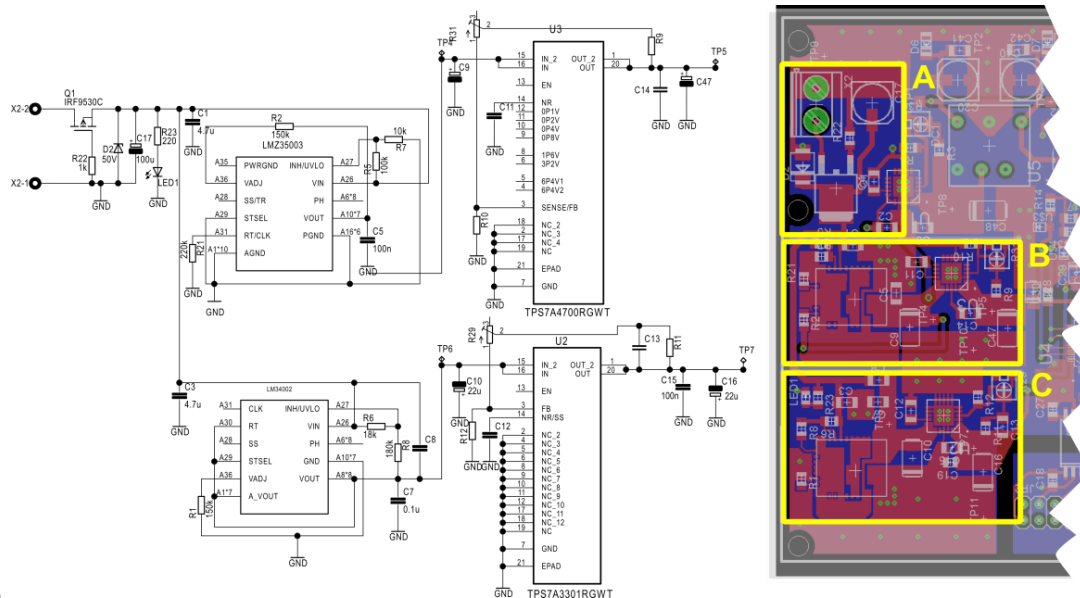


Figure 5: Schematic and layout of split-rail buck converter with marked: (A) Input voltage amplitude and reverse polarity protection circuit, B) Positive rail C) Negative rail.

The 24 VDC input voltage is then passed to a high performance regulated split-rail buck converter. Highly integrated **LMZ34002** and **LMZ35003** “Simple switchers™” modules were used to generate  $\pm 12.7$  V. They were chosen in favour of minimal number of external components, easy design and extremely small footprint. We optimized the switching design components using a **WEBENCH designer**, which served for initial design. To achieve optimal electrical and thermal performances, special care was given to maintain a proper PCB layout (Fig.5 right) – we used large

copper areas for power planes and multiple vias in order to minimize conduction losses and thermal stress. Low ESR tantalum capacitors were chosen and placed as close to the module pins as possible, in order to attenuate high frequency noise. Special attention was paid to the connection of analog and digital grounds at a single point – at pins 8 and 9. Output of the switching power supplies is further regulated by ultra-low noise LDOs **TPS7A4701** and **TPS7A3301**. Low ESR Tantalum capacitors were used near the ICs. By exploiting combination of integrated switcher and low-noise LDO, we came out with a highly integrated high performance power supply required for precision DAC power supply.

### 3.2.3 DAC and HV amplifier

The initial idea of piezo beam steering has first been tested using an **DAC8734EVM** evaluation board. After initial tests, we carefully studied the design of the EVM board and followed the same system concept in our design. In order to protect SPI communication lines, a capacitive galvanic isolation **ISO7240C** is used to accommodate for unidirectional isolation of CLK, CS, SDI and LATCH signals. 100 nF Tantalum capacitors were placed as close as possible to device terminals. At the isolated side, an additional UA78L05 was added to provide a logic level for both isolator and DAC.

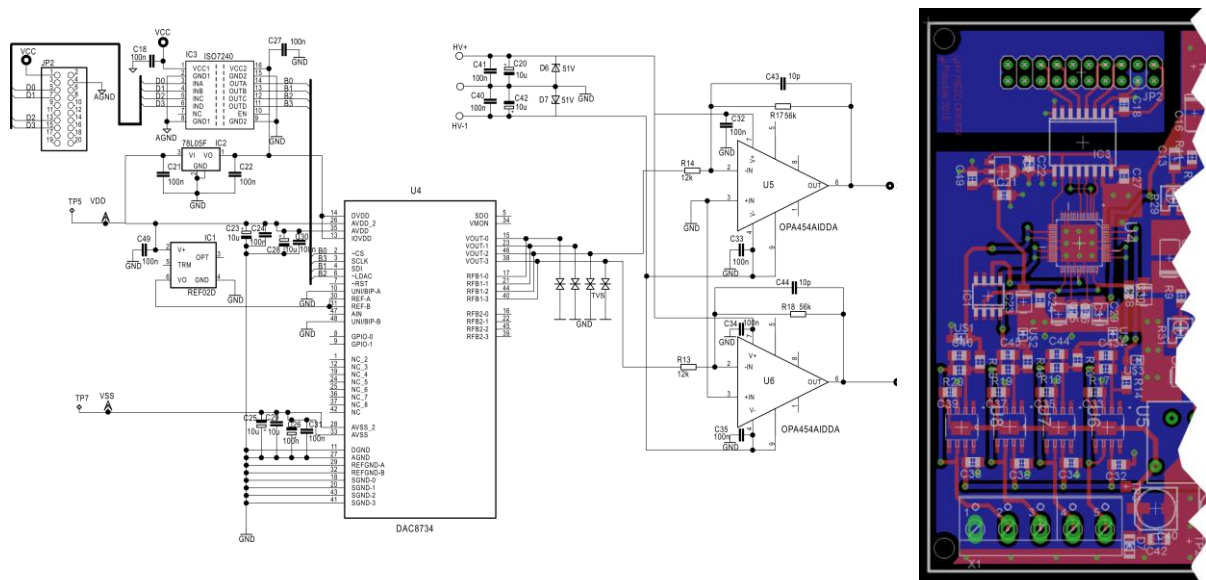


Figure 6: DAC design (Please note that two opamps are omitted on the schematic).

The DAC8734 is referenced by a 5.00 V low-noise precision voltage reference **REF02** supplied from 12 V positive rail. Bipolar ultralow noise  $\pm 12$  V split-rail power supply is used in order to provide enough power for  $\pm 10$  V output voltage swing. Transient voltage suppression diodes were added on the DAC outputs in order to protect DAC during slewing. The PCB layout of a precision DAC has to be done very carefully, if a good 16 bit precision is desired. Multiple vias were placed under the DAC to assure good grounding. We kept digital lines only 10 mils wide, whereas power planes were kept as wide as possible, with closely placed capacitors. At both rails, 100 nF ceramic capacitors parallel to 10 uF low ESR Tantalum capacitors are

placed against ground. Output channel lines were kept 25 mils wide in order to minimize voltage drops due to resistance.

The generated signals are fed to 4 channel HV amplifier. Here, 100 Vp-p **OPA454** were chosen for being the highest voltage opamps available at the market and capable of up to 50 mA output current, enough to power piezoelectric mirrors. At power rails two additional 51 V protection Zener diodes suppress potential overvoltages. The opamps are wired as negative feedback amplifiers, with gain set as  $-\frac{R_F}{R_i} = -4.66$ . Apart of using 1% resistors to minimize channel differences, their resistance were measured and the resistor pairs were first bench-tested and matched. Parallel to a feedback resistor, a 10pF capacitor was planned to limit the bandwidth, but was later found to be superfluous and was not added in final design.

### 3.2.3 Microcontroller and software

Position instructions are provided by a host computer running MathWorks Matlab. A necessary trajectory is generated and coordinates of desired geometry are sent over a high bandwidth USB interface using a custom protocol to a **MSP430F5529 Launchpad**. The MSP430 decodes the instructions, transforms the geometry to electrode voltages and sends it to DAC over a 24 MHz SPI. Two different system modes are implemented – *asynchronous mode* is used for instant responses to input instructions, where DAC update is executed as soon as the electrode voltages are updated from the instruction decoder input. For smoother beam steering along a predefined curve, *synchronous mode* is preferred. Here, instructions are first decoded and fed to a FIFO buffer. They are executed on Timer interrupt, triggered every 12  $\mu$ s. In a Timer ISR, the trajectory is iteratively interpolated in order to lower the number of required input coordinate and to decrease time spent on USB communication and instructions decoding. For this a fast iterative Bresenham interpolation algorithm was implemented. We ended up with a system design capable of high speed performance of 75000 updates/sec.

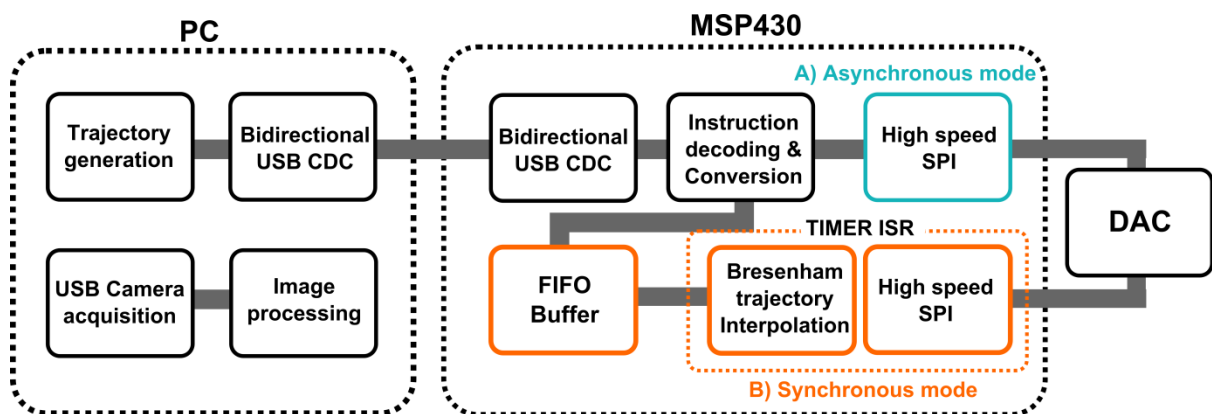


Figure 7: Software architecture



#### 4. Final application

Fig.8 shows individual system units and their integration into a prototype optical setup, built to verify the system performance. In setup a laser diode passing through linear polarizer and polarizing beam splitter illuminates the deformable mirror mounted at one arm of the system. The light bounces off the mirror and falls on a CMOS sensor of a camera mounted at the other side.

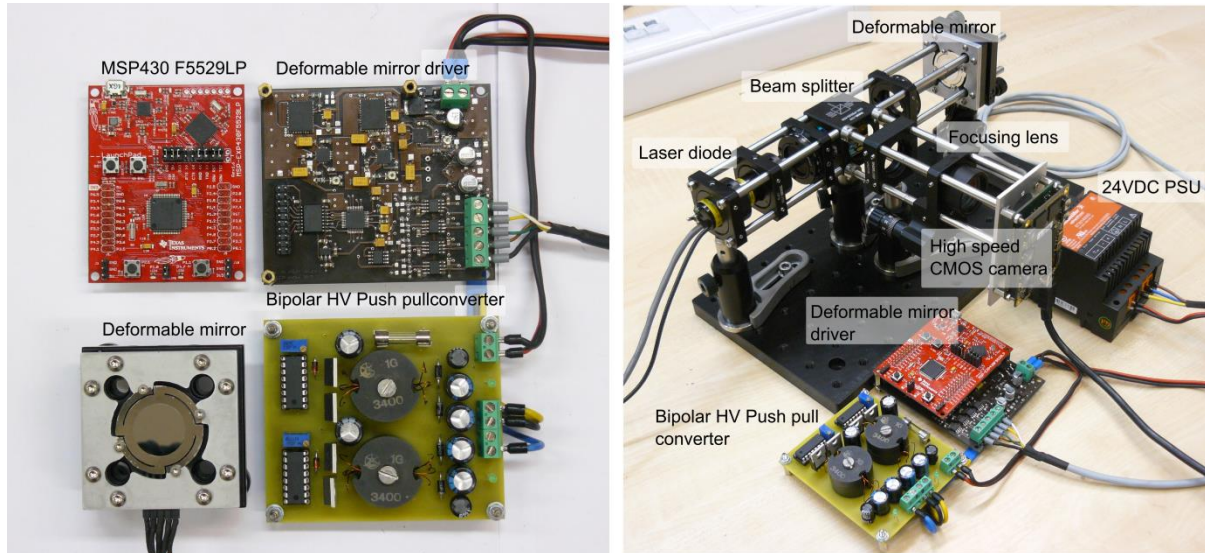


Figure 8: Individual system units (Left), Integration of the deformable mirror into an optical instrument prototype (Right)

The exact pixel size of a CMOS sensor ( $3.63 \mu\text{m}$  for Sony IMX035) allows precise spatial measurements of laser beam position. The camera and detection algorithm is capable of 120 Hz image streams, which was found enough for testing quasistatic and slow dynamic system performance. Unfortunately this measurement technique does not allow us to study the higher system dynamics, including mirror resonance behaviour.

#### 5. Experimental results

First, the electrical system response under load was measured. A reference signal of 23 V amplitude was set on output of a piezo amplifier, and voltage response on piezo actuator has been acquired (Fig.9). The output voltage settles in  $5 \mu\text{s}$ , overshoots less than 1.5 V and remains stable afterwards. Next what interests us the most, is the linearity of the deformable mirror system. Surprisingly, the deformable mirror exhibit perfect linear performance with

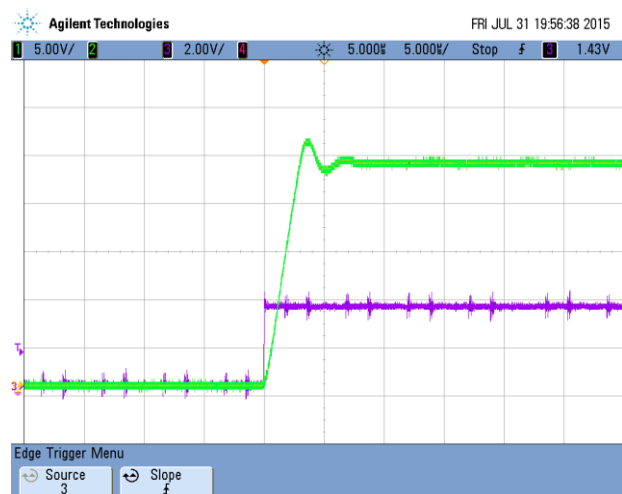


Figure 9: Electrical system response (shown in green) and trigger signal (shown in violet)

sensitivity coefficient measured to be  $\gamma = 0.022 \text{ mrad/V}$  and nonlinearities lower than  $0.9 \text{ mrad}$  over the whole working range of  $\pm 0.63^\circ$ . The nonlinearities mainly result from piezo hysteresis but remain under critical values. Since the deflection angles are small, the linearity is maintained even after the deflected light passes through the focusing optics. The focusing optics provides sharp focus and magnifies the working area to  $120 \times 120 \text{ }\mu\text{m}$ . To demonstrate system capabilities a **TI logo smaller than thickness of a human hair** has been drawn with a laser. First, an automatic edge detection algorithm was used to trace the geometry of the logo from a bitmap picture. The desired geometry consisting of 475 points was sent over to MSP430 where required voltages for each electrode were calculated and generated for each point. The CMOS sensor was used to measure the beam position. Fig. 10 shows the end results - the desired logo is smaller than a human hair; exploiting the limits of the employed measurement technique.

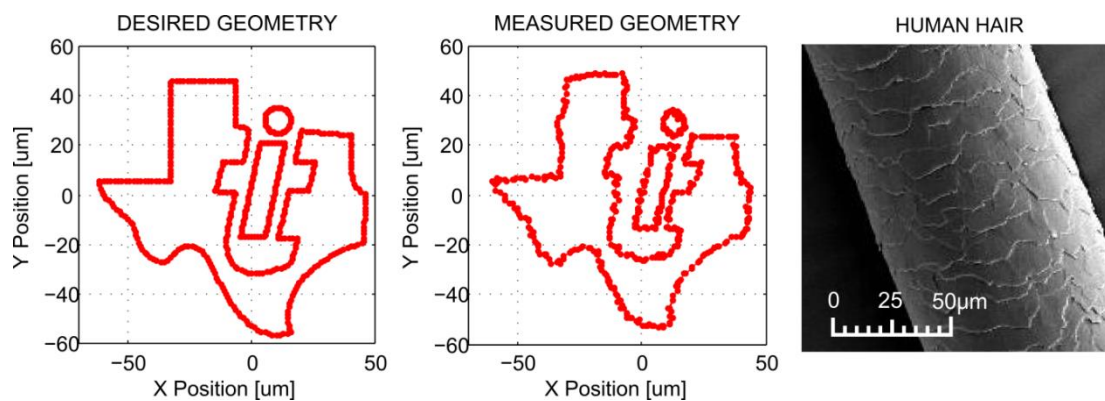


Figure 10 : Desired (left) and measured trajectory of laser beam (in the middle), steered by presented deformable mirror system. Human hair serves for size comparison (right).

## 5. Conclusion

The system performances exceeded all our initial expectations. Good system linearity and astonishing submicron steering capabilities have been demonstrated at 75 kpps speeds, which is opening numerous application possibilities.

## 6. Summary

This report outlines the development of an affordable high precision beam steering based on the principles of piezoelectric deformable mirror. Using TI's solutions, we were able to develop a high-tech device from scratch in an extremely short time period. During the design stage, **TI's evaluation boards** turned out to be the fastest way to test and bring the novel ideas to life. Next, the design was optimized and key components were found by exploiting a **Webench designer**. **Device datasheets** were found full of useful instructions and hints for a good layout. Finally, the **Code Composer Studio** with numerous useful code examples provided good base to start coding and bring the system to life.

## 7. Future plans

Beside further system improvements and testing, our future plans point towards integration of the deformable mirror system into a precision scanning confocal microscope, aimed for measuring 3D topography of microstructures.

## Bill of materials

Value	Quantity	Package	Manufacturer
R10	4	R0805	Multicomp
R27	2	R0805	Multicomp
R220	1	R0805	Multicomp
R390	1	R0805	Multicomp
R1k	5	R0805	Multicomp
R1.8k	2	R0805	Multicomp
R3.3k	2	R0805	Multicomp
C4.7k	2	R0805	Multicomp
C20k	2	R0805	Multicomp
C10n	4	C0805	Murata
C47n	2	C0805	Murata
C100n	2	C0805	Murata
CP10u	5	B/3528-21R	Kemet
CP100uF 63V	4	E5-10.5	Jamicon
CP470u 50V	2	E5-10.5	Jamicon
Zener 12V	2	DO34Z7	Panasonic
DZ436000	1	SMB	Panasonic
Fuse F800mA	1		Littelfuse
8.22mH	2	822J	Fastron
IRF540	4	TO220	International rectifier
UF4007	4	DO41	Fairchild semiconductors
UC3525A	2	DIP16	Texas Instruments
Connector	3	2 pin	Wago
Transformer 2.08	2	Ø26x26	Custom build
R1k	1	R0805	Multicomp
R2.2k	1	R0805	Multicomp
R10k	2	Trimmer	BOURNS
R12k	4	R0805	Multicomp
R18k	1	R0805	Multicomp
R56k	4	R0805	Multicomp
R62k	2	R0805	Multicomp
R100k	1	R0805	Multicomp
R150k	2	R0805	Multicomp
R220k	1	R0805	Multicomp
C10p	4	C0805	Murata
C10n	1	C0805	Murata
C100n	22	C0805	Murata
C1u	4	B/3528-21R	Kemet
C4.7u	2	B/3528-21R	Kemet
C10u	2	EU153CLV	Panasonic
C22u	1	EU153CLV	Panasonic
IRF9530	1	TO20	International rectifier
T12C	4	SOD323	Bourns
DZ436000	1	SMB	Panasonic
BZV55-C 51V	2	SOD80C	NXP
REF02D	1	SOIC8	TexasInstruments
UA78L05	1	SOT89	TexasInstruments
ISO7240C	1	SO-16Dw	TexasInstruments
TPS7A4701	1	QFN65P	Texas Instruments
TPS7A3301	1	QFN65P	Texas Instruments
LMZ34002	1	QFN41P	TexasInstruments
LMZ35003	1	QFN41P	TexasInstruments
DAC8734	1	QFP50P	Texas Instruments
OPA454	4	SOIC127	Texas Instruments
Connector	3	3-pin	Wago